Supplementary Information for

Geological modulation of N_2O emissions in rivers globally

Hongkai **Qi**[1,2,3], Yi **Liu**[1,2 *], Haoran **Wang**[1], Yu **Pang**[3], Junyu **Li**[3], Xiao **Ma**[4], Longjun **Wu**[2, 3], Ding **He**[2, 3], Jianping **Gan**[2, 3]

[1] Earth, Ocean and Atmospheric Sciences (EOAS) Thrust, Function Hub, The Hong Kong University of Science and Technology (Guangzhou), Guangzhou, China

[2] Center for Ocean Research in Hong Kong and Macau (CORE), Hong Kong, China

[3] Department of Ocean Science, The Hong Kong University of Science and Technology, Hong Kong, China

[4] School of Marine Sciences, Sun Yat-sen University, Zhuhai, China

[*]Corresponding author.

Contents of this file

- Supplementary Text 1 to 2
- Fig. S1 to S9

Text 1: Factors related to N_2O production besides water pH and sediment TOC

In the PRB, the overlying water dissolved oxygen (DO) is 5.95±1.58 mg/L in the PRB, which provides a relatively oxic environment for denitrification in the surface sediment. Overlying DO does not show a significant difference between the carbonate- and the silicate-dominated regions (6.52±1.36 mg/L vs. 6.16±1.73 mg/L, $p>0.05$, Fig. S6), eliminating DO been the key factor influencing N_2O production.

In addition, global riverine NO_3^- concentration is similar in carbonate- and silicate-dominated regions even though a little bit higher median NO_3^- in silicate-dominated rivers than their counterparts (21.2 μmol/L vs. 16.7 μmol/L, Fig. S7) is observed. This indicates that the nitrogen (N) inputs are comparably uniform for the regions with silicate-dominated and carbonate-dominated bedrocks worldwide. Moreover, riverine NH_4^+ is far lower than NO_3^-, with a mean NO_3^-:NH_4^+ ratio of 53.2 and a median ratio of 25.0 (calculated based on the GloRiCH database [1]), confirming the key role of denitrification rather than nitrification in riverine N_2O emission [2-4].

Text 2: N removal and N_2O production in the PRB with different geological backgrounds and yield budgets

With the measured potential denitrification rate (R_{DNT}), N_2O production rate (R_{N2O}), and area of the river [5] in the PRB, we estimates a potential N removal yield of 170-222 Gg N/yr and a N_2O production yield of 5-7 Gg N/yr in total (Extended Data Fig. 2). The N removal in the PRB accounted for 4%-6% of China's total N removal yield (3.8±1 Tg N/yr) in river system, even though the area of which only accounts for 2%-3%. This is consistent with our previous finding that the R_{DNT} in the PRB is the highest across China (more than double the national average value), owing to the high pollution [6]. Applying the average N fertilizer application rate in the PRB (35.42 kg N/ha/yr averaged during 1997 to 2008) [7] and the Intergovernmental Panel on Climate Change (IPCC) emission factor (30%) [8], 36%-47% of the leached N is removed through the complete denitrification process ($NO_3^- \rightarrow N_2$) in riverbed sediments, but 1.1%-1.5% of which is transformed as N_2O ($NO_3^- \rightarrow N_2O$). Since the emission factor in IPCC is generally deemed to be too high for estimating N leaching [9], the actual N removal and N_2O production percentages may be underestimated. In summary, the riverbed geology plays a critical role in controlling the basin-scale N budget and N_2O production.

In addition, N removal per unit area is the lower in the silicate-dominant region (53 Ton N/km^2/yr) compared to that in the carbonate-dominant region (68 Ton N/km^2/yr), while the N_2O production is over double in the silicate-dominant region (4.0 Ton N/km^2/yr) than its counterpart (1.6 Ton N/km^2/yr) (Extended Data Fig. 2). In addition, rivers in the silicate-dominant region account for 18.7% of the total fertilizer application, but the N removal only accounts for 12% regarding the entire PRB. In contrast, it represents 28.6% of the total N_2O production in the PRB, attributed to the combined effects of reduced residence time, sediment total organic carbon (TOC), and river water pH induced from distinct bedrock properties.

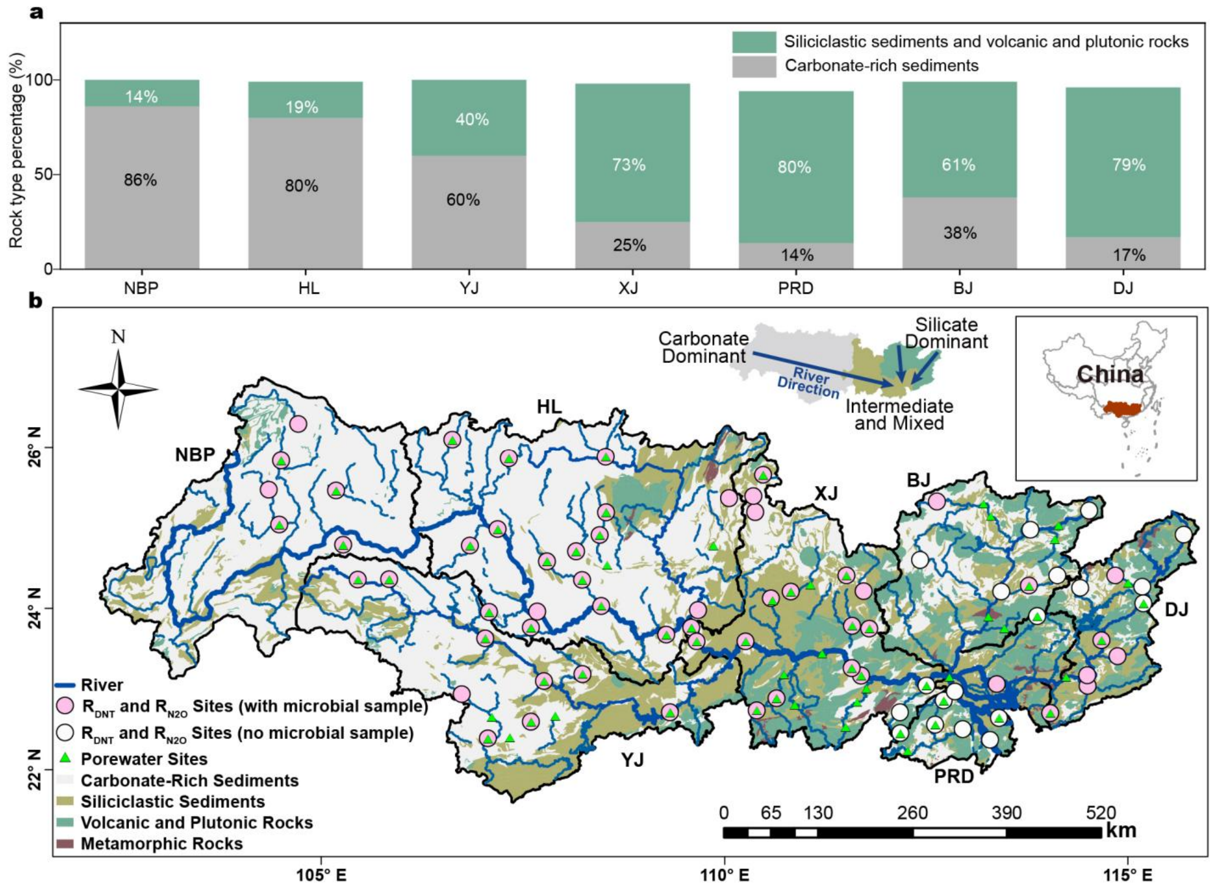

Fig. S1. Study area (PRB) and sampling sites. a, Rock type distribution across sub-basins. **b**, Study area geologic background and sampling sites. NBP=Nan-bei Pan River Basin, YJ=Yujiang River Basin, HL=Hongliu River Basin, XJ=Xijiang River Basin, BJ=Beijiang River Basin, DJ=Dongjiang River Basin, PRD=Pearl River Delta.

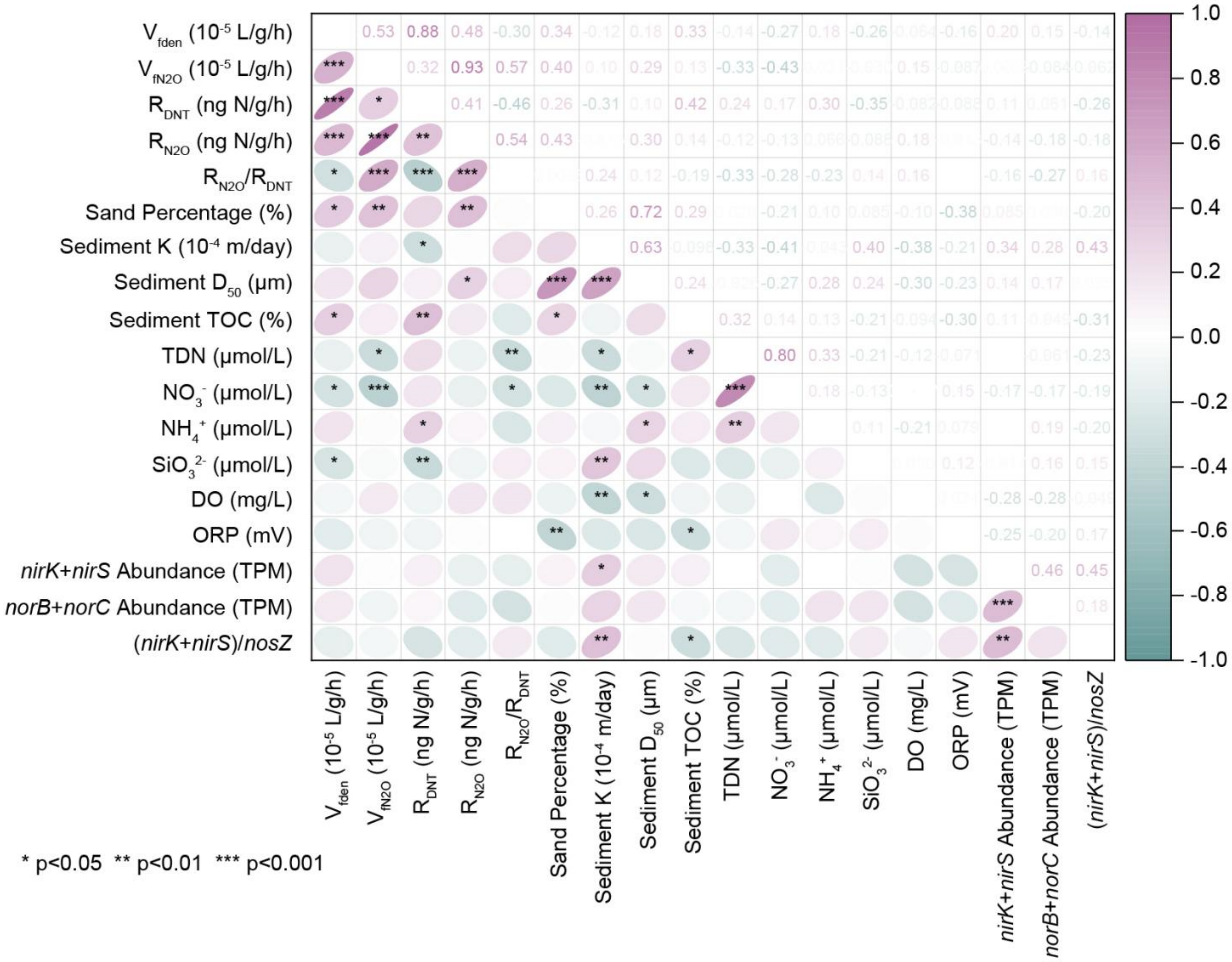

Fig. S2. Spearman correlation between potential denitrification rate (R_{DNT}), nitrous oxide production rate (R_{N2O}), and variables. *p*<0.001 represents extremely significant, *p*<0.01 represents highly significant, *p*<0.05 represents significant, otherwise there is no statistical significance. V_{fden}=the uptake rate N through denitrification, V_{fden}=the uptake rate N through N_2O production, TOC=total organic carbon, K=sediment hydraulic conductivity, D_{50}=median grain size, TDN=total dissolved nitrogen in overlying water, NO_3^-=nitrate in overlying water, NH_4^+=ammonium in overlying water, SiO_3^{2-}=silicate in overlying water, DO=dissolved oxygen in overlying water), ORP=oxidation-reduction potential of overlying water. The numbers represent the Spearman correlation coefficient.

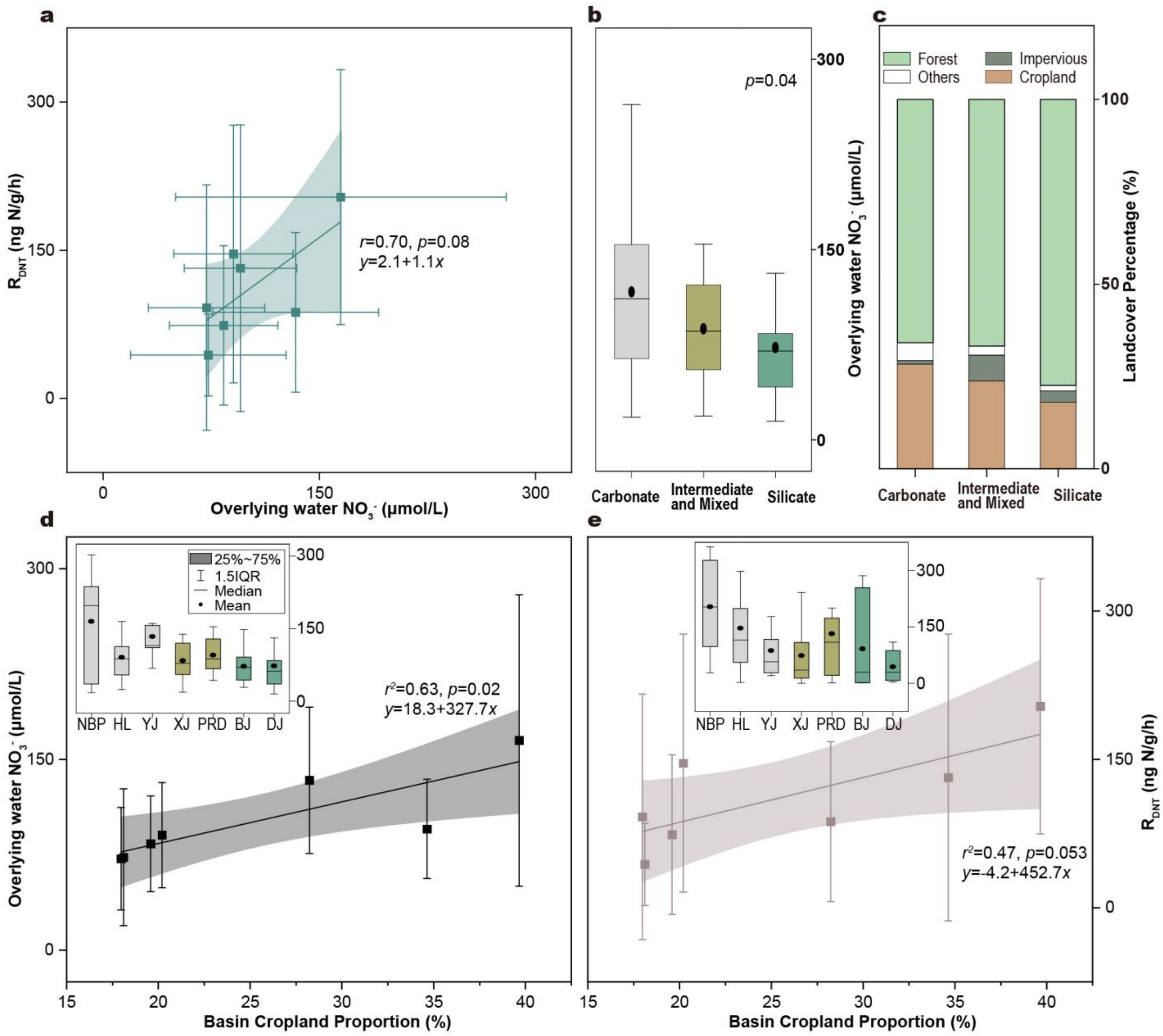

Fig. S3. Basin-scale overlying water NO_3^- and R_{DNT} distribution and relationship with basin cropland proportion. **a,** correlation of overlying water NO_3^- and R_{DNT}. **b,** overlying water NO_3^- zonation across regions with different geologic backgrounds. **c,** landcover types across regions with different geologic backgrounds. **d,** overlying water NO_3^- variation across basins and correlation with basin cropland proportion. **e,** R_{DNT} variation with basins and correlation with basin cropland proportion. The square dots in **a, d,** and **e** represent the mean values, and the error bar represents the standard deviations. The linear lines and shadows represent the linear regression and the 95% confidence bands. For the box plots in **b, d**, and **e**, the black points, black line inside the box, and whiskers outside the boxes represent the mean value, median value, and 1.5 interquartile range (IQR), respectively. Two-sided Kruskal-Wallis Test is applied in the comparison in **b**, where $p<0.01$ represents highly significant, $p<0.05$ represents significant, otherwise there is no statistical significance.

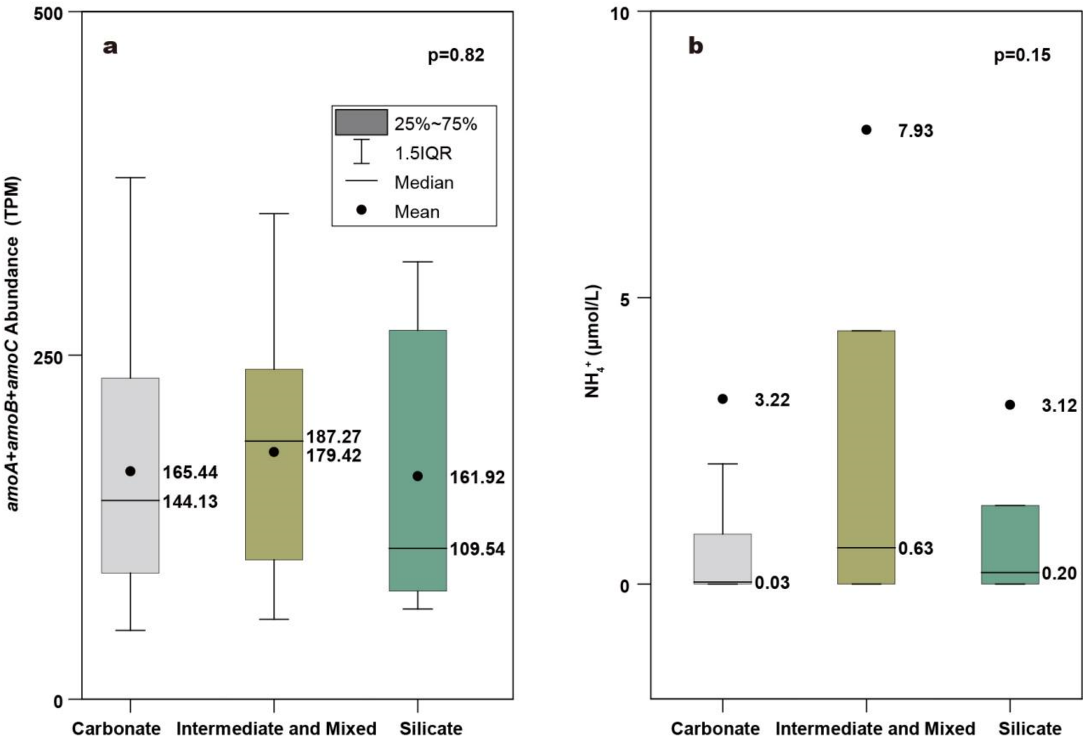

Fig. S4. Comparison of ammonia-oxidizing genes' abundance and ammonium (NH_4^+) across rivers with different geologic backgrounds. a, the variation of the total abundance of *amoA*, *amoB*, *amoC*. **b,** the variation of NH_4^+. Two-sided Kruskal-Wallis Test is applied in the comparison, where $p<0.01$ represents highly significant, $p<0.05$ represents significant, otherwise there is no statistical significance. The black points, black line inside the box, and lines outside the boxes represent the mean value, median value, and 1.5 IQR, respectively. The numbers beside the black point and median line represent the mean and median values, respectively.

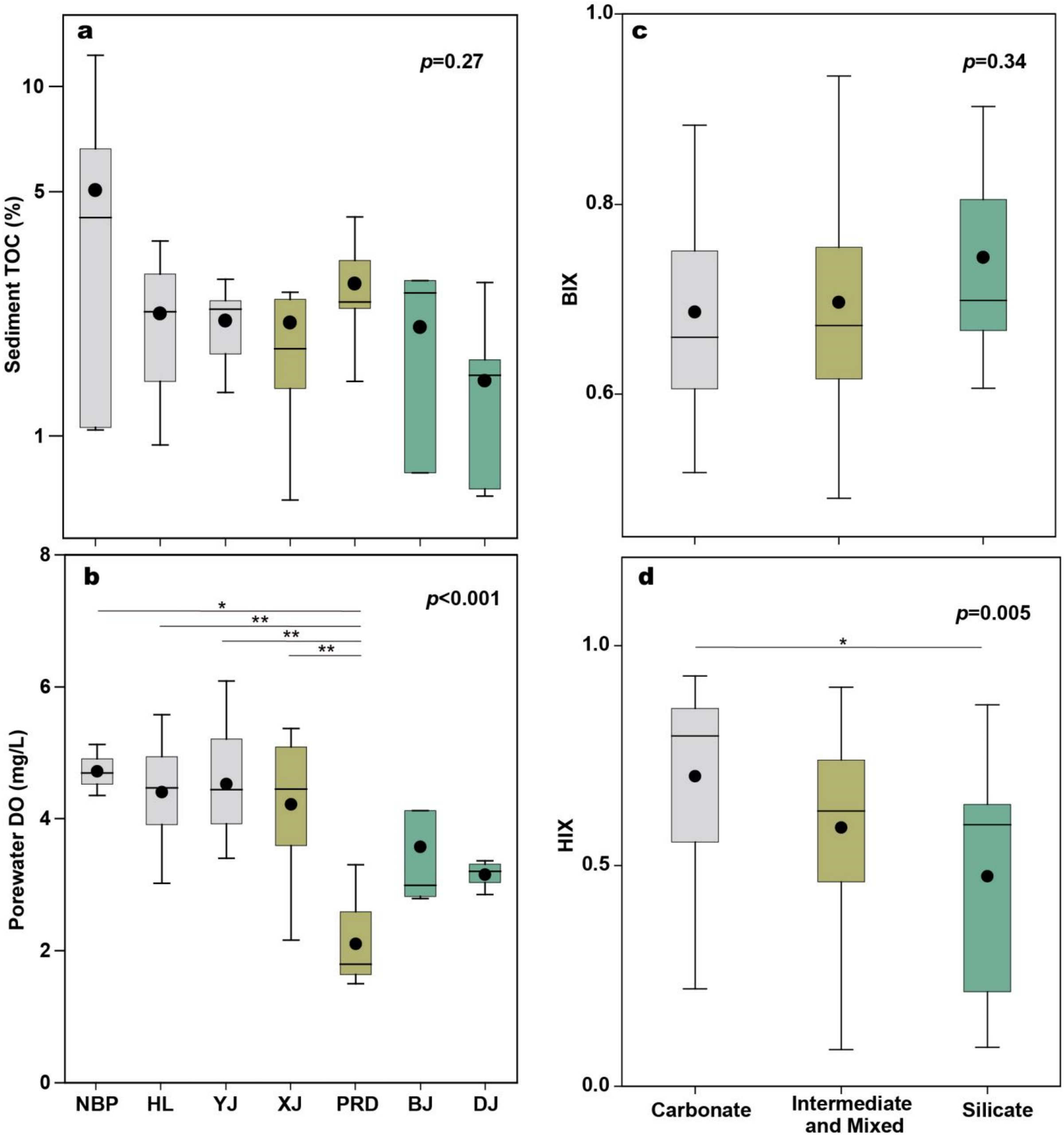

Fig. S5. Variations of Sediment TOC, porewater DO, sediment water-extractable dissolved organic matter (DOM) biological index (BIX), and sediment water-extractable DOM humification index (HIX) in the PRB. a, **b**, Sediment TOC (a) and porewater DO (b) across sub-basins. **c**, **d**, Sediment water extractable DOM BIX (c) and HIX (d) across regions with different geologic backgrounds. Two-sided Kruskal-Wallis Test is applied in the comparison between groups, and “*” represents a significant difference ($p<0.05$), and “**” represents a highly significant difference ($p<0.01$), otherwise there is no statistical significance. The black points, black line inside the box, and lines outside the boxes represent the mean value, median value, and 1.5 IQR, respectively.

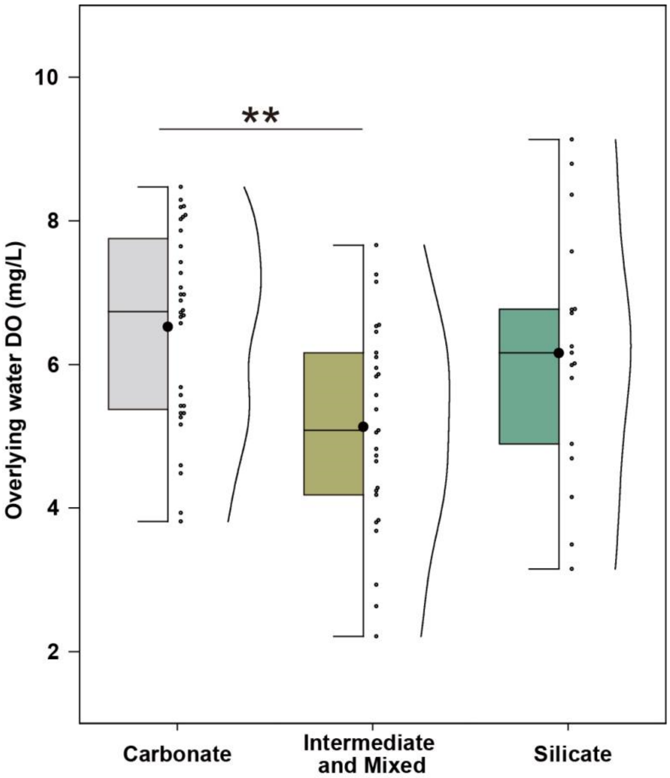

Fig. S6. Overlying water DO across different regions. Two-sided Kruskal-Wallis Test is applied in the comparison between groups, and "*" represents a significant difference (p<0.05), and "**" represents a highly significant difference (p<0.01), otherwise there is no statistical significance. The black points, black line inside the box, and lines outside the boxes represent the mean value, median value, and 1.5 IQR, respectively. The dots and the curves beside the boxes represent the data and the data distribution.

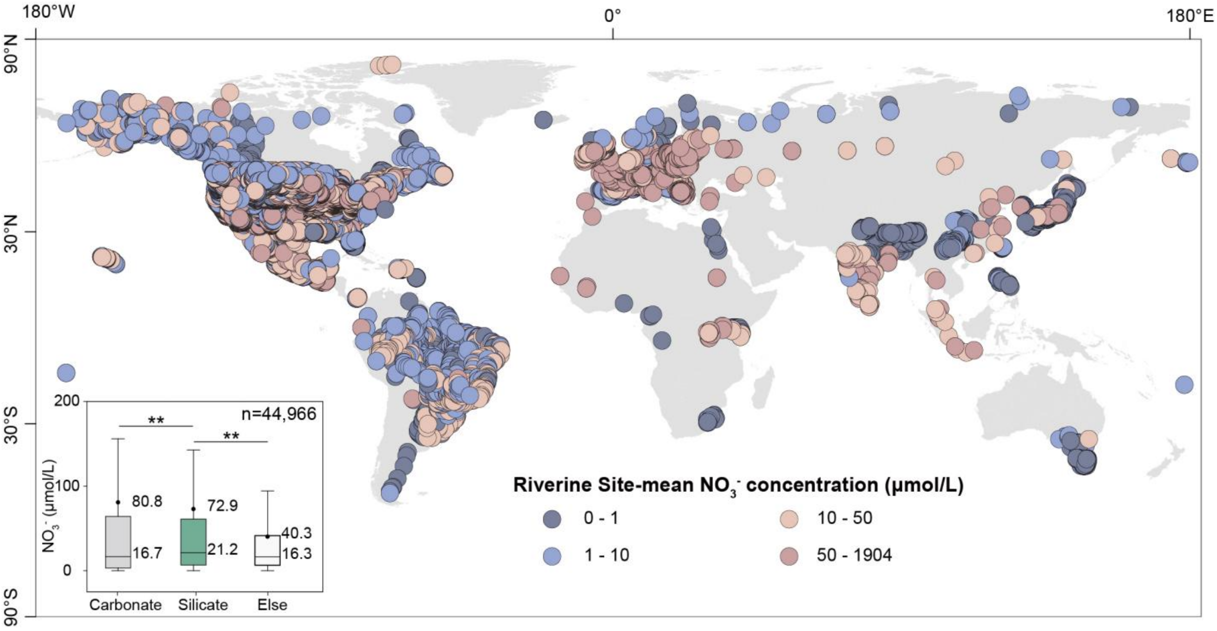

Fig. S7. Global Riverine NO_3^- distribution and comparison across different geology. The values are the mean site values calculated from the GRQA database [10]. For the box plot, the black points, the black line inside the boxes, whiskers outside the boxes, and the dots outside of the whiskers represent the mean value, median value, 1.5 IQR, and the outliers respectively. Two-sided Kruskal-Wallis Test is applied in the comparison between groups, and "*" represents significant difference (p<0.05), and "**" represents highly significant difference (p<0.01), otherwise there is no statistical significance.

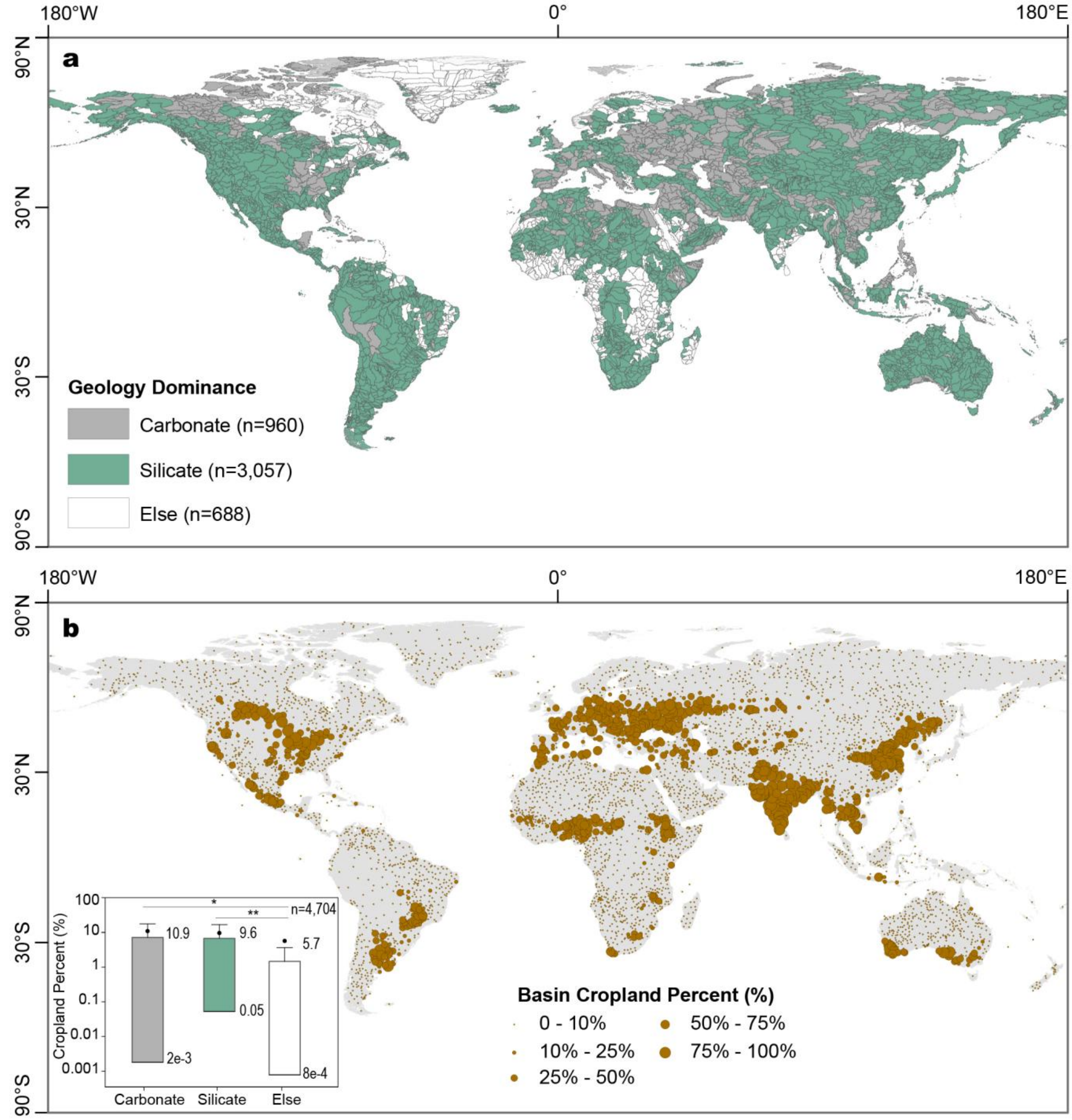

Fig. S8. Global calculation of geology dominance and cropland percentage across basins. a, Global geology dominance across the basins calculated based on HydroBASINS (level 05) [11] and the GLiM database [12]. **b,** Global basin-scale cropland percentage (based on the global MCD12Q1 landcover database [13]) and zonation according to different geologic backgrounds. The black points, the black line inside the boxes, whiskers outside the boxes, and the dots outside of the whiskers represent the mean value, median value, 1.5 IQR, and the outliers, respectively. Two-sided Kruskal-Wallis Test is applied in the comparison between groups, and "*" represents a significant difference (p<0.05), and "**" represents a highly significant difference (p<0.01), otherwise there is no statistical significance.

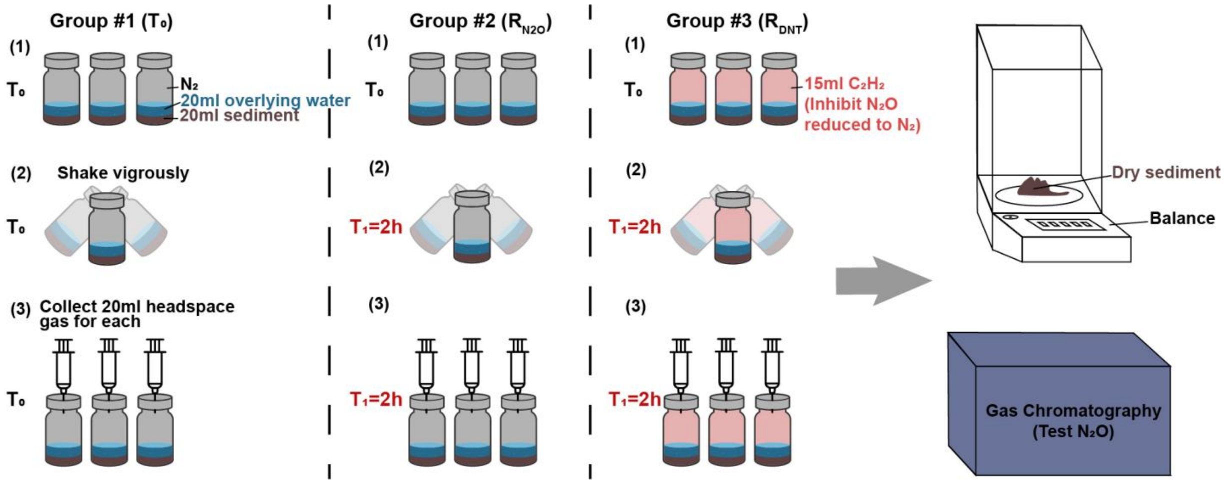

Fig. S9. Schematic diagram of incubation experiment settings to obtain the R_{DNT} and R_{N2O}.

References

1 Hartmann, J., Lauerwald, R. & Moosdorf, N. in *Supplement to: Hartmann, J et al. (2014): A Brief Overview of the GLObal RIver Chemistry Database, GLORICH. Procedia Earth and Planetary Science, 10, 23-27, https://doi.org/10.1016/j.proeps.2014.08.005* (PANGAEA, 2019).

2 Yao, Y., Tian, H., Shi, H., Pan, S., Xu, R., Pan, N. & Canadell, J. G. Increased global nitrous oxide emissions from streams and rivers in the Anthropocene. *Nature Climate Change* **10**, 138-142, doi:10.1038/s41558-019-0665-8 (2020).

3 Beaulieu, J. J., Tank, J. L., Hamilton, S. K., Wollheim, W. M., Hall, R. O., Mulholland, P. J., Peterson, B. J., Ashkenas, L. R., Cooper, L. W., Dahm, C. N., Dodds, W. K., Grimm, N. B., Johnson, S. L., McDowell, W. H., Poole, G. C., Valett, H. M., Arango, C. P., Bernot, M. J., Burgin, A. J., Crenshaw, C. L., Helton, A. M., Johnson, L. T., O'Brien, J. M., Potter, J. D., Sheibley, R. W., Sobota, D. J. & Thomas, S. M. Nitrous oxide emission from denitrification in stream and river networks. *Proceedings of the National Academy of Sciences* **108**, 214-219, doi:10.1073/pnas.1011464108 (2011).

4 Marzadri, A., Dee, M. M., Tonina, D., Bellin, A. & Tank, J. L. Role of surface and subsurface processes in scaling N2O emissions along riverine networks. *Proceedings of the National Academy of Sciences* **114**, 4330-4335, doi:10.1073/pnas.1617454114 (2017).

5 Gu, C., Liu, Y., Qi, H. & Lu, M. Influences of carbonate weathering and hyporheic exchange on carbon fluxes in Pearl River Basin, China. *Water Research* **261**, 122014, doi:https://doi.org/10.1016/j.watres.2024.122014 (2024).

6 Qi, H. & Liu, Y. Nitrogen removal through denitrification in China's aquatic system. *Science of The Total Environment* **891**, 164317, doi:https://doi.org/10.1016/j.scitotenv.2023.164317 (2023).

7 Yu, Z., Liu, J. & Kattel, G. Historical nitrogen fertilizer use in China from 1952 to 2018. *Earth Syst. Sci. Data* **14**, 5179-5194, doi:10.5194/essd-14-5179-2022 (2022).

8 IPCC. Guidelines for national greenhouse gas inventories. *Prepared by the National Greenhouse Gas Inventories Programme. Eggleston HS, Buendia L, Miwa K, Ngara T, Tanabe K, editors. Published: IGES, Japan* (2006).

9 Wang, Y., Ying, H., Yin, Y., Zheng, H. & Cui, Z. Estimating soil nitrate leaching of nitrogen fertilizer from global meta-analysis. *Science of The Total Environment* **657**, 96-102, doi:https://doi.org/10.1016/j.scitotenv.2018.12.029 (2019).

10 Virro, H., Amatulli, G., Kmoch, A., Shen, L. & Uuemaa, E. GRQA: Global River Water Quality Archive. *Earth Syst. Sci. Data* **13**, 5483-5507, doi:10.5194/essd-13-5483-2021 (2021).

11 Lehner, B. & Grill, G. Global river hydrography and network routing: baseline data and new approaches to study the world's large river systems. *Hydrological Processes* **27**, 2171-2186, doi:https://doi.org/10.1002/hyp.9740 (2013).

12 Hartmann, J. & Moosdorf, N. The new global lithological map database GLiM: A representation of rock properties at the Earth surface. *Geochemistry, Geophysics, Geosystems* **13**, doi:https://doi.org/10.1029/2012GC004370 (2012).

13 Friedl, M. & Sulla-Menashe, D. MCD12Q1 MODIS/Terra+Aqua Land Cover Type Yearly L3 Global 500m SIN Grid V006. *NASA Land Processes Distributed Active Archive Center. Date Accessed: 2025-09-22* (2019).